

# One-dimensional rarefactive solitons in electron-hole semiconductor plasmas

Yunliang Wang<sup>1</sup> and Bengt Eliasson<sup>2</sup><sup>1</sup>*Department of Physics, School of Mathematics and Physics, University of Science and Technology Beijing, Beijing 100083, China*<sup>2</sup>*SUPA, Physics Department, John Anderson Building, University of Strathclyde, Glasgow G4 0NG, United Kingdom*

(Received 9 March 2014; revised manuscript received 25 April 2014; published 27 May 2014)

We present a theory for linear and nonlinear excitations in semiconductor quantum plasmas consisting of electrons and holes. The system is governed by two coupled nonlinear Schrödinger equations for the collective wave functions of the electrons and holes and Poisson's equation for the electrostatic potential. This gives a closed system including the effects of charge separation between the electrons and holes, quantum tunneling, quantum statistics, and exchange correlation due to electron spin. Three typical semiconductors, GaAs, GaSb, and GaN, are studied. For small-amplitude excitations, the dispersion relation reveals the existence of one high-frequency branch due to charge-separation effects and one low-frequency branch due to the balance between pressure and inertia of the electrons and holes. For the fully nonlinear excitations, the profiles of quasistationary soliton solutions are obtained numerically and show depleted electron and hole densities correlated with a localized potential. The simulation results show that the rarefactive solitons are stable and can withstand perturbations and turbulence for a considerable time.

DOI: [10.1103/PhysRevB.89.205316](https://doi.org/10.1103/PhysRevB.89.205316)

PACS number(s): 52.35.Mw, 73.22.Lp, 52.40.Db

## I. INTRODUCTION

Modern semiconductor quantum devices, such as spintronics, nanotubes, quantum dots, and quantum wells [1,2], work with electrons and holes at nanometer scales [3]. The interaction of intense laser pulses with matter can create electron-hole plasmas at high densities [4], where electrons transit from the valence to the conduction band after absorbing the photon energy by single- or multiphoton absorption with holes created in the valence band. Recently, experiments and simulations have shown the existence of moving bright cavity polariton solitons propagating across the semiconductor microcavity [5,6]. The formation and properties of bright polariton solitons in semiconductor microcavities operating in the strong-coupling regime are affected by the exciton-photon coupling due to electron-hole pair screening [7]. Experimental observations of acoustic solitons have also been made in a GaAs slab at low temperature with a picosecond acoustic technique [8], and fully developed acoustic solitons have also been observed in several crystalline solids [9]. Quantum dispersion effects associated with electron oscillations have been observed experimentally in metals [10] and in warm dense plasmas [11]. Semiconductors provide a compact and inexpensive medium to observe the quantum dispersion effects. In miniature semiconductor devices, the quantum effects are very important since the de Broglie thermal wavelength of the charged carriers can be comparable to the characteristic spatial scales of the system [12], and since the electrons and holes are fermions, they obey the Fermi-Dirac statistics. Hence, the effects of quantum tunneling and degeneracy pressure have to be taken into account for electron-hole quantum semiconductor plasmas [13–15]. The presence of quantum effects reduces the threshold electric field for the onset of parametric amplification, and accordingly, the pump electric field can easily be achieved in unmagnetized *n*-type piezoelectric semiconductors [16]. The quantum effects may also lead to quasiquantum lattices of colloid ions at quantum scales [17].

The formation of solitons is due to a balance between dispersion and nonlinearity. In electron-hole semiconductor quantum plasmas, the dispersion effects are due to charge

separation between the electrons and holes and due to quantum recoil, and the nonlinearities are due to the large-amplitude electrostatic potential as well as the quantum degeneracy pressure and the exchange-correlation potential [18–22]. By using quantum hydrodynamic equations [23] for electrons and holes, bright solitons have been investigated theoretically for several kinds of semiconductors [24]. It has also been shown that quantum electron oscillation can support the formation of stable dark (rarefactive) solitons and vortices [25] associated with localized positive potentials.

In this paper, we investigate the linear and nonlinear properties of semiconductor plasmas with electrons and holes as charge carriers, particularly the possibility of localized nonlinear structures in the form of solitons. The solitons are characterized by a local depletion of the electron and hole densities, accompanied by a large-amplitude localized electrostatic potential, and are formed due to the combined effects of charge separation, quantum tunneling, quantum statistical pressure, and exchange correlations due to spin.

## II. DYNAMICAL MODEL OF ELECTRON-HOLE SEMICONDUCTOR PLASMAS

Using the translational symmetry in the transverse plane, we here consider the one-dimensional propagation in the *x* direction of nonlinear electrostatic acoustic waves in a semiconductor plasma consisting of equal amounts of electrons and holes. To model the dynamics of the electrons and holes in the semiconductor, we use the nonlinear Schrödinger equation (NLSE) for the electrons and holes,

$$i \frac{\partial \psi_e}{\partial t} + H_e \frac{\partial^2 \psi_e}{\partial x^2} + (\Gamma_{xce} \phi_{xce} + \phi - \Gamma_e |\psi_e|^4) \psi_e = 0, \quad (1)$$

$$i \frac{\partial \psi_h}{\partial t} + H_h \frac{\partial^2 \psi_h}{\partial x^2} + (\Gamma_{xch} \phi_{xch} - \phi - \Gamma_h |\psi_h|^4) \psi_h = 0, \quad (2)$$

where  $\psi_e$  and  $\psi_h$  are the collective wave functions of the electrons and holes, respectively, normalized by  $\sqrt{n_0}$ , where  $n_0$  is the equilibrium electron and hole number density. The quantum parameter  $H_{e,h} = \hbar^2 \omega_{pe,ph}^2 / 2E_{Fe}^2$  determines

the relative importance of the quantum electron/hole recoil effects, where  $\omega_{pe,ph} = (4\pi n_0 e^2 / \epsilon m_{e,h}^*)^{1/2}$  is the electron/hole plasma frequency and  $E_{Fe,Fh} = \hbar^2 (3\pi^2 n_0)^{2/3} / 2m_{e,h}^*$  is the electron/hole Fermi energy. Here  $\epsilon$  is the relative dielectric constant of the material,  $e$  is the magnitude of the electron charge, and  $m_{e,h}^*$  is the effective electron/hole mass. The interactions between the electrons and holes are governed by the exchange correlation and electrostatic (Hartree) potentials. The third term,  $\Gamma_{xce,xch} \phi_{xce,xch} \psi_{e,h}$ , is due to the electron/hole exchange-correlation potential [18], where  $\Gamma_{xce} = \Gamma_{xch} = 0.985 e^2 / \epsilon r_0 E_{Fe}$  and  $r_0 = n_0^{-1/3}$  is the Wigner-Seitz radius. Hence, the normalized potentials are  $\phi_{xce,xch} = -[|\psi_{e,h}|^{2/3} + \alpha_{e,h} \ln(1 + \beta_{e,h} |\psi_{e,h}|^{2/3})]$ , where  $\alpha_{e,h} = 0.034 / a_{Be,Bh}^*$  and  $\beta_{e,h} = 18.37 a_{Be,Bh}^*$ , with  $a_{Be,Bh}^* = \epsilon \hbar^2 / m_{e,h}^* e^2 r_0$  being the Bohr radius divided by the Wigner-Seitz radius [18,19,21,22]. The term  $\Gamma_{e,h} |\psi_{e,h}|^4 \psi_{e,h}$  originates from the quantum statistical electron/hole Fermi pressure  $P_{e,h} = m_{e,h}^* V_{Fe,Fh}^2 n_0 / 3(n_{e,h} / n_0)^3$  [19,23,25], with  $V_{Fe,Fh} = (2E_{Fe,Fh} / m_{e,h}^*)^{1/2}$  being the Fermi speed [23] and where the corresponding effective potential is repulsive. Here  $\Gamma_{e,h} = E_{Fe,Fh} / E_{Fe}$  is a dimensionless constant, and  $n_{e,h} = |\psi_{e,h}|^2$  is the electron/hole number density normalized by  $n_0$ . The space and time coordinates are normalized by  $\lambda_{DFe} = (E_{Fe} / 4\pi e^2 n_0)^{1/2}$  and  $\hbar / E_{Fe}$ , respectively, and the potential is normalized by  $E_{Fe} / e$ . Equations (1) and (2) are closed by Poisson's equation

$$\frac{\partial^2 \phi}{\partial x^2} = |\psi_e|^2 - |\psi_h|^2 \quad (3)$$

for the electrostatic potential. Equations (1)–(3) govern the collective electron and hole oscillations due to the charge separation between electrons and holes. We stress that Eqs. (1) and (2) for the dynamics of the electrons and holes include the combined effects of the electron and hole quantum tunneling, the quantum statistical pressures, and exchange and correlation effects due to spin. At short wavelengths, the quantum effects become important and give rise to dispersion effects in the electrostatic wave.

The particular forms of Eqs. (1) and (2) are due to the formulation of Manfredi and Haas [23], who derived a collective Schrödinger equation for an ensemble of electrons. We briefly describe this formalism here. Starting from a multistream kinetic model for the electrons, where each stream is governed by a single-particle Schrödinger equation, the continuity and momentum equations are derived by taking the moments of the electron distribution function and using a fluid closure based on equal amplitudes of each stream. Finally, assuming a curl-free electron fluid velocity and employing ideas similar to the ones of Madelung [26] and Bohm [27], the quantum fluid equations for the electron number density and velocity are transformed to a NLSE for a complex-valued, collective electron wave function. Using the formalism of Ref. [23] for electrons and holes would result in Eqs. (1) and (2) without the exchange-correlation potential but including the electrostatic potential  $\phi$  and the electron and hole pressure terms proportional to  $|\psi_e|^4$  and  $|\psi_h|^4$ . The latter are the degeneracy pressures, derived from the second moments of the electron and hole distribution functions, and are assumed to be purely one-dimensional Fermi-Dirac distributions in the cold limit. (In  $D$  dimensions,

the pressure terms would instead be proportional to  $|\psi_e|^{4/D}$  and  $|\psi_h|^{4/D}$  [23].) Since the underlying fluid equations have curl-free velocities, vortices can exist in multiple dimensions only in the form of point vortices, where the density goes to zero at the center of the vortex [28]. The interaction of vortices in two dimensions exhibits pairing of vortices and stability only for vortices with topological charge (circulation number) equal to  $\pm 1$  [25,29]. Finally, the exchange-correlation potentials are taken to be in the form given by Brey *et al.* [18] based on a parametrization suggested by Hedin and Lundqvist [30]. The formalism of the collective Schrödinger equation and application of the exchange-correlation potential for electrons is further discussed in Ref. [19]. In the present model, the electrons and holes are interacting only via the electrostatic (Hartree) potential, while further collective electron-electron and hole-hole interactions take place via the respective exchange-correlation potentials and degeneracy pressures. Hence, the dynamics of electrons and holes are included in our model on an equal footing, which is useful for the investigation of spintronics, nanotubes, quantum dots, and quantum wells, where electrons and holes interact on nanometer scales.

In the numerical examples below, we will consider three typical semiconductors [1,3,14,24], (i) GaAs with the parameters  $n_0 = 4.7 \times 10^{16} \text{ cm}^{-3}$ ,  $m_h^* = 0.5m_e$ ,  $m_e^* = 0.067m_e$ , and  $\epsilon = 12.8$ ; (ii) GaSb with the parameters  $n_0 = 1.6 \times 10^{17} \text{ cm}^{-3}$ ,  $m_h^* = 0.4m_e$ ,  $m_e^* = 0.047m_e$ , and  $\epsilon = 15.69$ ; and (iii) GaN with the parameters  $n_0 = 1 \times 10^{20} \text{ cm}^{-3}$ ,  $m_h^* = 1.3m_e$ ,  $m_e^* = 0.13m_e$ , and  $\epsilon = 11.3$ . For GaAs we then have  $H_e = 9.603$ ,  $H_h = 1.287$ ,  $\lambda_e = 0.174$ ,  $\lambda_h = 0.736$ ,  $\Gamma_e = 1$ ,  $\Gamma_h = 0.134$ , and  $\Gamma_{xce} = \Gamma_{xch} = 0.563$ ; for GaSb we have  $H_e = 4.478$ ,  $H_h = 0.526$ ,  $\lambda_e = 0.276$ ,  $\lambda_h = 0.768$ ,  $\Gamma_e = 1$ ,  $\Gamma_h = 0.117$ , and  $\Gamma_{xce} = \Gamma_{xch} = 0.214$ ; and for GaN we have  $H_e = 1.448$ ,  $H_h = 0.145$ ,  $\lambda_e = 0.761$ ,  $\lambda_h = 1.522$ ,  $\Gamma_e = 1$ ,  $\Gamma_h = 0.100$ , and  $\Gamma_{xce} = \Gamma_{xch} = 0.096$ .

### III. LINEAR WAVE SPECTRUM

We first investigate the linear properties of the system (1)–(3). The equilibrium solution of the system (1)–(3) is given by  $\psi_e = \psi_{e0}$ ,  $\psi_h = \psi_{h0}$ , and  $\phi = 0$ , where  $\psi_{e0}$  and  $\psi_{h0}$  are complex constants such that  $|\psi_{e0}|^2 = |\psi_{h0}|^2 = 1$  and where the frequencies are  $\Omega_{e0} = -(\Gamma_{xce} \phi_{xce0} - \Gamma_e)$  and  $\Omega_{h0} = -(\Gamma_{xch} \phi_{xch0} - \Gamma_h)$ . The system is linearized by perturbing the equilibrium and setting  $\psi_e = (\psi_{e0} + \psi_{e1}) \exp(-i\Omega_{e0}t)$ ,  $\psi_h = (\psi_{h0} + \psi_{h1}) \exp(-i\Omega_{h0}t)$ , and  $\phi = \phi_1$ , where it is assumed that  $|\psi_{e1}| \ll |\psi_{e0}|$  and  $|\psi_{h1}| \ll |\psi_{h0}|$ . The linearized equations are then given by

$$i \frac{\partial \psi_{e1}}{\partial t} + H_e \frac{\partial^2 \psi_{e1}}{\partial x^2} - \left[ \frac{1}{3} \Gamma_{xce} \left( 1 + \frac{\alpha_e \beta_e}{1 + \beta_e} \right) + 2\Gamma_e \right] \times (\psi_{e1} + \psi_{e0}^* \psi_{e1}^*) + \psi_{e0} \phi_1 = 0, \quad (4)$$

$$i \frac{\partial \psi_{h1}}{\partial t} + H_h \frac{\partial^2 \psi_{h1}}{\partial x^2} - \left[ \frac{1}{3} \Gamma_{xch} \left( 1 + \frac{\alpha_h \beta_h}{1 + \beta_h} \right) + 2\Gamma_h \right] \times (\psi_{h1} + \psi_{h0}^* \psi_{h1}^*) - \psi_{h0} \phi_1 = 0, \quad (5)$$

$$\frac{\partial^2 \phi_1}{\partial x^2} = \psi_{e0} \psi_{e1}^* + \psi_{e0}^* \psi_{e1} - (\psi_{h0} \psi_{h1}^* + \psi_{h0}^* \psi_{h1}). \quad (6)$$

Next, the first-order quantities are represented by Fourier modes as  $\psi_{e1} = \widehat{\psi}_{e+} \exp(iKx - i\Omega t) + \widehat{\psi}_{e-} \exp(-iKx + i\Omega t)$ ,  $\psi_{h1} = \widehat{\psi}_{h+} \exp(iKx - i\Omega t) + \widehat{\psi}_{h-} \exp(-iKx + i\Omega t)$ , and  $\phi_1 = \widehat{\phi} \exp(iKx - i\Omega t) + \widehat{\phi}^* \exp(-iKx + i\Omega t)$ , where  $\Omega$  and  $K$  are the frequency and wave number, respectively, of the electrostatic oscillations. Inserting these Fourier representations into the linearized equations (4)–(6) and separating different Fourier modes and eliminating the Fourier coefficients, we obtain the dispersion relation for the electrostatic oscillations as

$$1 + \frac{1}{D_{Le}} + \frac{1}{D_{Lh}} = 0, \quad (7)$$

where contributions of the electron and hole oscillations are given, respectively, by

$$D_{Le} = -\frac{\Omega^2}{2H_e} + \frac{1}{2}H_e K^4 + \frac{1}{3} \left( \frac{C_{xce}^2}{C_{se}^2} + 3 \frac{V_{Fe}^2}{C_{se}^2} \right) K^2, \quad (8)$$

$$D_{Lh} = -\frac{\Omega^2}{2H_h} + \frac{1}{2}H_h K^4 + \frac{1}{3} \left( \frac{C_{xch}^2}{C_{sh}^2} + 3 \frac{V_{Fh}^2}{C_{sh}^2} \right) K^2, \quad (9)$$

where  $C_{xce}^2 = 0.985(1 + 0.62/18.37a_{Be}^*)e^2/\epsilon r_0 m_e^*$ ,  $C_{xch}^2 = 0.985(1 + 0.62/18.37a_{Bh}^*)e^2/\epsilon r_0 m_h^*$ ,  $C_{se}^2 = E_{Fe}/m_e^*$ , and  $C_{sh}^2 = E_{Fh}/m_h^*$ . We note that the dispersion of the quantum electron oscillation  $1 + D_{Le} = 0$  is identical to that obtained by the NLSE-Poisson system in a quantum plasma with degenerate electron fluids [31] if the effects of charge exchange and correlation are neglected. We numerically solve the dispersion relation of the semiconductor quantum plasmas and display the results in Fig. 1. We notice from Fig. 1 that the system supports both high-frequency electrostatic oscillations, similar to plasma oscillations in classical electron-positron or electron-ion plasmas, and low-frequency acoustic-like oscillations. The high-frequency plasma oscillations are primarily due to charge separation, where the electrons and holes oscillate against each other with opposite phases, while the low-frequency acoustic-like oscillations are due to a balance

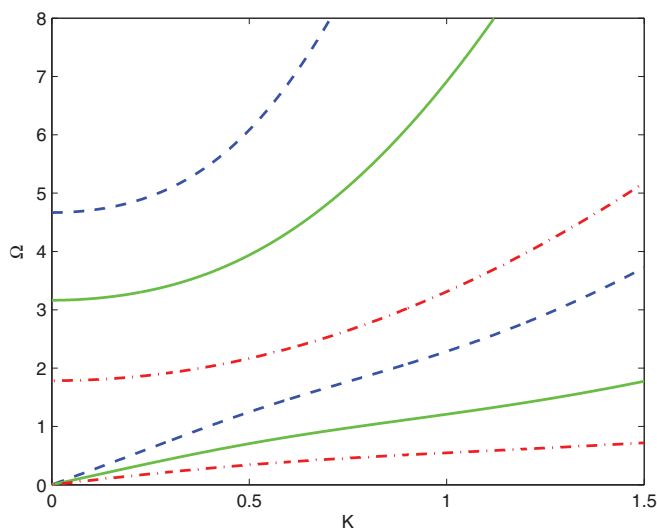


FIG. 1. (Color online) Wave dispersion curves for GaAs (blue dashed line), GaSb (green solid line), and GaN (red dash-dotted line) semiconductor plasmas.

between pressure and inertia, where the electrons and holes oscillate with the same phases.

#### IV. THE EXISTENCE AND STABILITY OF QUASISTATIONARY RAREFACTIVE SOLITONS

We next investigate the possibility of nonlinear excitations governed by the system (1)–(3). To model nonlinear quasistationary structure moving with a constant speed  $v_0$ , we introduce the ansatz  $\psi_e = W_e(\xi) \exp(iK_e x - i\Omega_e t)$ ,  $\psi_h = W_h(\xi) \exp(iK_h x - i\Omega t)$ , and  $\phi = \phi(\xi)$  into Eqs. (1)–(3), where  $W_e$  and  $W_h$  are real-valued functions of the argument  $\xi = x - v_0 t$ . The quantities  $K_{e,h}$  and  $\Omega_{e,h}$  of the electrostatic waves are constant wave number and frequency shifts, respectively. By choosing  $K_e = v_0/2H_e$  and  $K_h = v_0/2H_h$ , Eqs. (1)–(3) can be written as

$$\frac{\partial^2 W_e}{\partial \xi^2} + \lambda_e W_e + \frac{1}{H_e} (\Gamma_{xce} \phi_{xce} + \phi - \Gamma_e W_e^4) W_e = 0, \quad (10)$$

$$\frac{\partial^2 W_h}{\partial \xi^2} + \lambda_h W_h + \frac{1}{H_h} (\Gamma_{xch} \phi_{xch} - \phi - \Gamma_h W_h^4) W_h = 0, \quad (11)$$

$$\frac{\partial^2 \phi}{\partial \xi^2} = W_e^2 - W_h^2, \quad (12)$$

where  $\lambda_e = \Omega_e/H_e - K_e^2$  and  $\lambda_h = \Omega_h/H_h - K_h^2$  are eigenvalues of the system. From the boundary conditions  $|W_e| = 1$ ,  $|W_h| = 1$ , and  $\phi = 0$  at  $|\xi| = \infty$ , we obtain  $\lambda_e = \Gamma_e/H_e - \Gamma_{xce} \phi_{xce0}/H_e$ ,  $\lambda_h = \Gamma_h/H_h - \Gamma_{xch} \phi_{xch0}/H_h$ ,  $\Omega_e = \Gamma_e + v_0^2/4H_e - \Gamma_{xce} \phi_{xce0}$ , and  $\Omega_h = \Gamma_h + v_0^2/4H_h - \Gamma_{xch} \phi_{xch0}$ , where the exchange-correlation potentials at equilibrium are  $\phi_{xce0} = -[1 + (0.034/a_{Be}^*) \ln(1 + 18.37a_{Be}^*)]$  and  $\phi_{xch0} = -[1 + (0.034/a_{Bh}^*) \ln(1 + 18.37a_{Bh}^*)]$ .

We solved the system (10)–(12) as a nonlinear boundary-value problem with the boundary conditions  $W_e = -1$  on the left boundary  $\xi = -10$ ,  $W_e = +1$  on the right boundary  $\xi = 10$ , and  $W_h = 1$  on both the left and right boundaries. The potential  $\phi$  is set to zero at the two boundaries. The spatial domain is numerically resolved with 1000 intervals, and the second derivatives in the system (10)–(12) are approximated by centered second-order approximations. The resulting nonlinear system of equations is then solved numerically using Newton's method. The numerical solutions are displayed in Fig. 2. As seen in Fig. 2, the local depletions of the electron and hole densities are associated with a positive potential. The electron density goes to zero at the center of the solitons due to the choice of boundary conditions where the electron wave function has a phase shift and changes sign at the center of the solitons. The wave function of the holes is assumed to be the same phase at the left and right boundaries, and since the positively charged holes are repelled by the positive potential, the hole density is also decreased, but not completely depleted, at the center of the solitons.

In order to assess the dynamics and stability of the rarefactive solitons, we have solved the time-dependent system of Eqs. (1)–(3) numerically. We use a pseudospectral method for calculating the spatial derivatives with periodic boundary conditions and the standard fourth-order Runge-Kutta method to advance the solution in time. The spatial domain is from  $x = -5\pi$  to  $x = +15\pi$  with 512 intervals in space.

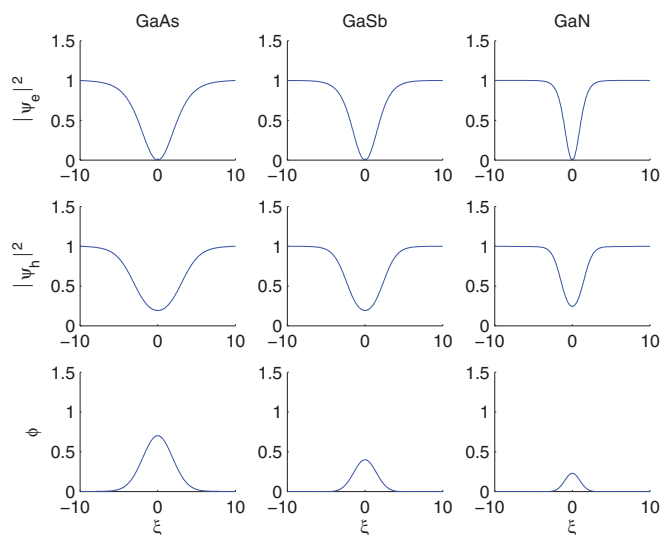


FIG. 2. (Color online) The spatial profiles of (top) the electron number density  $n_e = |\psi_e|^2$ , (middle) the hole number density  $n_h = |\psi_h|^2$ , and (bottom) the scalar potential  $\phi$  for rarefactive solitons in GaAs, GaSb, and GaN semiconductor plasmas (left to right columns, respectively).

We do the simulation from time  $t = 0$  to  $t = 20$  with the time step being  $\Delta t = 0.00001$ . The initial conditions are  $\psi_e = \tanh[20 \sin(x/10)]$  and  $\psi_h = 1$ , which is consistent with the periodic boundary conditions used in the simulations. In Figs. 3–5, the space and time evolutions of the electron and hole densities are displayed together with the potential for the GaAs, GaSb, and GaN cases, respectively. For the GaAs semiconductor, Figs. 3(a) and 3(b) show that the soliton withstands perturbations and turbulence for a considerable time. The width of the depletion of  $|\psi_e|^2$  is larger than that of  $|\psi_h|^2$ , which is consistent with the quasistationary solutions illustrated in Fig. 2. For GaSb, Fig. 4 shows that the soliton also survives perturbations and turbulence throughout

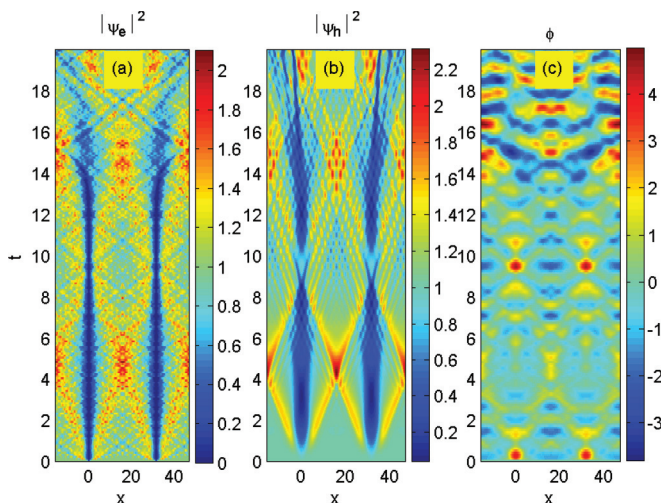


FIG. 3. (Color online) Nonlinear evolution of solitons in a GaAs semiconductor plasma: (a) the electron number density  $n_e = |\psi_e|^2$ , (b) the hole number density  $n_h = |\psi_h|^2$ , and (c) the scalar potential  $\phi$ .

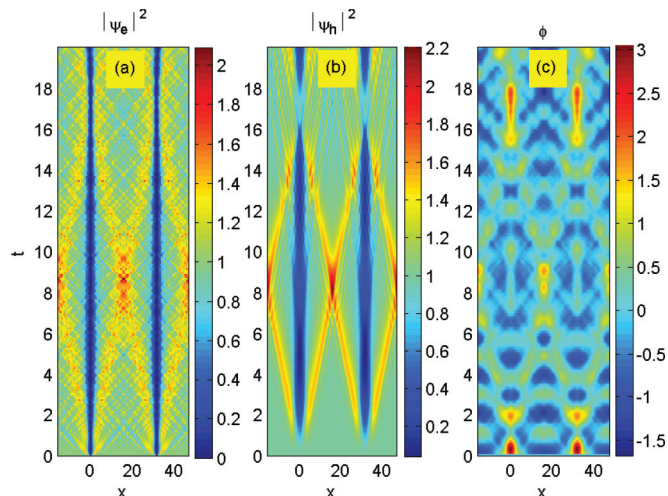


FIG. 4. (Color online) Nonlinear evolution of solitons in a GaSb semiconductor plasma: (a) the electron number density  $n_e = |\psi_e|^2$ , (b) the hole number density  $n_h = |\psi_h|^2$ , and (c) the scalar potential  $\phi$ .

the simulation. The soliton width in the GaSb semiconductor plasma is smaller than that for the GaAs semiconductor, which is also consistent with the quasistationary results in the left and middle columns in Fig. 2. Finally, for the semiconductor GaN, Fig. 5 shows that the widths of the local depletions of  $|\psi_e|^2$  and  $|\psi_h|^2$  in the GaN semiconductor plasma are smaller than for GaAs and GaSb and the solitons in GaN seem to be more stable than in GaAs and GaSb.

In Figs. 3–5, the simulations show that acoustic-like waves propagate away from the initial soliton profile with a speed that is highest for GaAs and lowest for GaN. The low-frequency dispersion curves in Fig. 1 also confirm that the acoustic speed is highest for GaAs and lowest for GaN. The right columns in Figs. 3–5 also show clearly visible electron-hole plasma oscillations in the potential. In the simulations, the

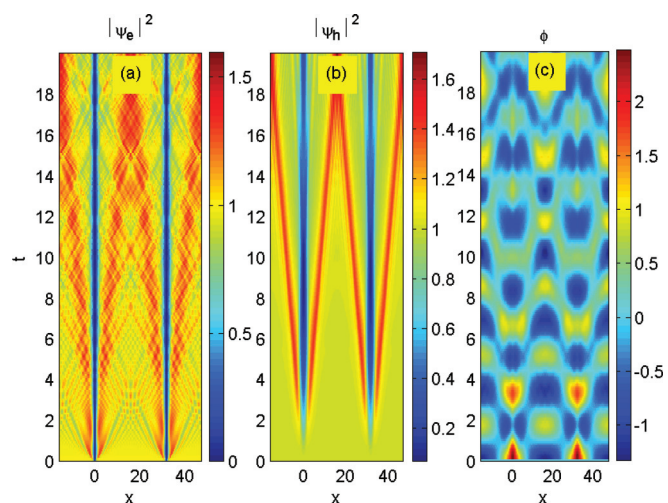


FIG. 5. (Color online) Nonlinear evolution of solitons in a GaN semiconductor plasma: (a) the electron number density  $n_e = |\psi_e|^2$ , (b) the hole number density  $n_h = |\psi_h|^2$ , and (c) the scalar potential  $\phi$ .

plasma oscillations have the highest frequency for the GaAs semiconductor plasma, while the GaN semiconductor has the lowest plasma oscillation frequency. The high-frequency plasma oscillations in the simulations are compatible with the high-frequency dispersion curves in Fig. 1. The amplitude of the localized potential associated with the solitary waves is largest for GaAs and smallest for GaN, which is consistent with the potential shown in the bottom row in Fig. 2.

## V. SUMMARY AND CONCLUSIONS

We have investigated the properties of linear and nonlinear quantum electrostatic acoustic waves in an electron-hole semiconductor quantum plasma taking into account the combined effects of the quantum recoil, the degenerate pressure effects, and the exchange-correlation potential due to spin. The dynamics of the system is governed by two coupled NLSEs for the collective wave functions of the electrons and holes and Poisson's equation for the Hartree potential. The interactions

also include the effects of the exchange-correlation potential due to the particle's spin.

By Fourier representations the dispersion relations give two wave modes, the Langmuir mode and the acoustic mode, which shows that the acoustic waves can propagate in semiconductor plasma due to the mass difference between the electrons and holes. A model for quasi-steady-state propagating quantum electrostatic waves is also derived, from which rarefactive solitons were numerically obtained. The numerical simulations show that the solitons are stable and can withstand perturbations and turbulence for a considerable time.

## ACKNOWLEDGMENTS

This research is partially supported by NSFC (Grant No. 11104012) and the Fundamental Research Funds for the Central Universities (Grants No. FRF-TP-09-019A and No. FRF-BR-11-031B).

- 
- [1] G. Manfredi and P.-A. Hervieux, *Appl. Phys. Lett.* **91**, 061108 (2007).
  - [2] F. Haas, G. Manfredi, P. K. Shukla, and P.-A. Hervieux, *Phys. Rev. B* **80**, 073301 (2009).
  - [3] K. Seeger, *Semiconductor Physics*, 9th ed. (Springer, Berlin, 2004).
  - [4] M. Combescot and J. Bok, *J. Lumin.* **30**, 1 (1985).
  - [5] A. Amo, D. Sanvitto, F. P. Laussy, D. Ballarini, E. del Valle, M. D. Martin, A. Lemaitre, J. Bloch, D. N. Krizhanovskii, M. S. Skolnick, C. Tejedor, and L. Vina, *Nature (London)* **457**, 291 (2009).
  - [6] O. A. Egorov, D. V. Skryabin, A. V. Yulin, and F. Lederer, *Phys. Rev. Lett.* **102**, 153904 (2009).
  - [7] O. A. Egorov, D. V. Skryabin, and F. Lederer, *Phys. Rev. B* **82**, 165326 (2010).
  - [8] E. Péronne and B. Perrin, *Ultrasonics* **44**, e1203 (2006).
  - [9] H.-Y. Hao and H. J. Maris, *Phys. Rev. B* **64**, 064302 (2001).
  - [10] H. Watanabe, *J. Phys. Soc. Jpn.* **11**, 112 (1956).
  - [11] S. H. Glenzer, O. L. Landen, P. Neumayer, R. W. Lee, K. Widmann, S. W. Pollaine, R. J. Wallace, G. Gregori, A. Höll, T. Bornath, R. Thiele, V. Schwarz, W.-D. Kraeft, and R. Redmer, *Phys. Rev. Lett.* **98**, 065002 (2007).
  - [12] P. K. Shukla and B. Eliasson, *Rev. Mod. Phys.* **83**, 885 (2011).
  - [13] A. P. Misra, *Phys. Rev. E* **83**, 057401 (2011).
  - [14] I. Zeba, M. E. Yahia, P. K. Shukla, and W. M. Moslem, *Phys. Lett. A* **376**, 2309 (2012).
  - [15] M. E. Yahia, I. M. Azzouz, and W. M. Moslem, *Appl. Phys. Lett.* **103**, 082105 (2013).
  - [16] S. Ghosh, S. Dubey, and R. Vanshpal, *Phys. Lett. A* **375**, 43 (2010).
  - [17] I. Zeba, Ch. Uzma, M. Jamil, M. Salimullah, and P. K. Shukla, *Phys. Plasmas* **17**, 032105 (2010).
  - [18] L. Brey, J. Dempsey, N. F. Johnson, and B. I. Halperin, *Phys. Rev. B* **42**, 1240 (1990).
  - [19] N. Crouseilles, P.-A. Hervieux, and G. Manfredi, *Phys. Rev. B* **78**, 155412 (2008).
  - [20] Y. Ma, S. Mao, and J. Xue, *Phys. Plasmas* **18**, 102108 (2011).
  - [21] P. K. Shukla, B. Eliasson, and L. Stenflo, *Phys. Rev. E* **86**, 016403 (2012).
  - [22] P. K. Shukla and B. Eliasson, *Phys. Rev. Lett.* **108**, 165007 (2012).
  - [23] G. Manfredi and F. Haas, *Phys. Rev. B* **64**, 075316 (2001).
  - [24] W. M. Moslem, I. Zeba, and P. K. Shukla, *Appl. Phys. Lett.* **101**, 032106 (2012).
  - [25] P. K. Shukla and B. Eliasson, *Phys. Rev. Lett.* **96**, 245001 (2006).
  - [26] E. Madelung, *Z. Phys.* **40**, 332 (1926).
  - [27] D. Bohm, *Phys. Rev.* **85**, 166 (1952).
  - [28] S. K. Ghosh and B. M. Deb, *Phys. Rep.* **92**, 1 (1982).
  - [29] I. A. Ivonin, V. P. Pavlenko, and H. Persson, *Phys. Rev. E* **60**, 492 (1999).
  - [30] L. Hedin and B. I. Lundqvist, *J. Phys. C* **4**, 2064 (1971).
  - [31] D. Pines, *Phys. Rev.* **92**, 626 (1953); D. Bohm and D. Pines, *ibid.* **92**, 609 (1953).